Polymer Chemistry

COMMUNICATION

Cite this: *Polym. Chem.*, 2015, **6**, 514

Received 8th October 2014,
Accepted 27th October 2014

DOI: 10.1039/c4py01373e

www.rsc.org/polymers

Accelerated living cationic ring-opening polymerization of a methyl ester functionalized 2-oxazoline monomer†

Petra J. M. Bouten,‡[a,b] Dietmar Hertsen,‡[c] Maarten Vergaelen,[a] Bryn D. Monnery,[a] Marcel A. Boerman,[b] Hannelore Goossens,[c] Saron Catak,[c,d] Jan C. M. van Hest,[b] Veronique Van Speybroeck*[c] and Richard Hoogenboom*[a]

Kinetic studies on the homo- and copolymerization of 2-methoxycarboxyethyl-2-oxazoline (MestOx) with 2-methyl-2-oxazoline (MeOx) and 2-ethyl-2-oxazoline (EtOx) were performed. For the homopolymerisation of MestOx an increased propagation rate constant was observed compared to MeOx and EtOx while the copolymerization of MestOx with MeOx or EtOx unexpectedly revealed slower incorporation of MestOx. Density functional theory (DFT) calculations show that nearby MestOx residues in the living chain can activate both the oxazolinium chain end and the attacking monomer, stabilizing the propagation transition state, leading to faster homopolymerisation of MestOx. These effects also accelerate incorporation of both monomers in the copolymerisations. However, since MeOx is shown to be more nucleophilic than MestOx, the incorporation order is reversed in the copolymerisations.

Poly(2-alkyl/aryl-oxazoline)s (PAOx) are an interesting class of polymers because of their tuneable properties, biocompatibility, stealth behaviour and thermosensitivity.[1–3] The living cationic ring-opening polymerisation (CROP) of 2-oxazoline monomers was first reported in the 1960s[4–7] providing an easy access to a wide variety of well-defined PAOx with controlled end-group functionality.[1,8–12] The properties of PAOx can be tuned by variation of the side chain substituent. Side chain functionalities, often protected, are mainly introduced during the 2-oxazoline monomer synthesis yielding functional PAOx by CROP.[13–22] PMeOx and PEtOx are of special interest for biomedical applications by their biocompatibility and stealth behaviour that is similar to poly(ethylene glycol) (PEG).[1,2,23]

Methyl ester functionalized side chains are especially interesting as they can be hydrolyzed to the carboxylic acid, a versatile functionality for conjugation of peptides and proteins, as well as the introduction of pH responsive behaviour. Moreover, PAOx with side chain methyl ester groups can undergo direct amidation with a variety of functional amines to easily introduce functional moieties in the side chain, such as amine, alcohol or hydrazide units.[24] Even though the synthesis and polymerization of 2-methoxycarbonyl-ethyl-2-oxazoline, a methyl ester containing oxazoline monomer (MestOx; Scheme 1), was already first reported by Levy and Litt in 1968[13] and this monomer has also been used more recently by the groups of Nuyken and Voit,[13–18] the (co)polymerisation kinetics of MestOx are yet unknown.

In this contribution we describe an improved synthesis method for MestOx (**1**) as well as detailed kinetic studies on the homo- and copolymerisation behaviour of MestOx with MeOx (**2**) and EtOx (**3**) revealing an unexpected effect of the MestOx side chain.

MestOx can be prepared in two steps from the commercially available methyl succinyl chloride (Scheme 2). At first methyl succinyl chloride (**1a**) is reacted with 2-chloroethylamine hydrochloride in presence of triethylamine, yielding the intermediate compound **1b** in 83% yield after purification. The MestOx monomer (**1**) is then obtained by ring closure of this linear precursor (**1b**) with a mild base, namely sodium carbonate, to avoid saponification of the ester. This ring-closing reaction is cumbersome due to the high viscosity of the reaction mixture in combination with the heterogeneity of the used salt

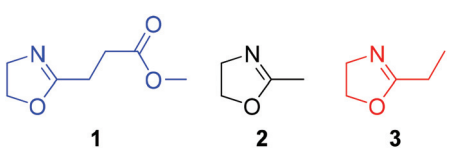

Scheme 1 Structures of MestOx (1), MeOx (2) and EtOx (3).

[a]*Supramolecular Chemistry Group, Department of Organic and Macromolecular Chemistry, Ghent University, Krijgslaan 281 S4, 9000 Ghent, Belgium. E-mail: richard.hoogenboom@ugent.be, veronique.vanspeybroeck@ugent.be*
[b]*Radboud University Nijmegen, Institute for Molecules and Materials (IMM), Heijendaalseweg 135, 6525 AJ Nijmegen, The Netherlands*
[c]*Center for Molecular Modeling (CMM), Ghent University, Technologiepark 903, Zwijnaarde 9052, 9000 Ghent, Belgium*
[d]*Bogazici University, Department of Chemistry, Bebek 34342 Istanbul, Turkey*

†Electronic supplementary information (ESI) available: Detailed experimental and theoretical methodology, Cartesian coordinates of all structures, interaction energies. See DOI: 10.1039/c4py01373e

‡These authors contributed equally to this work and share first authorship.

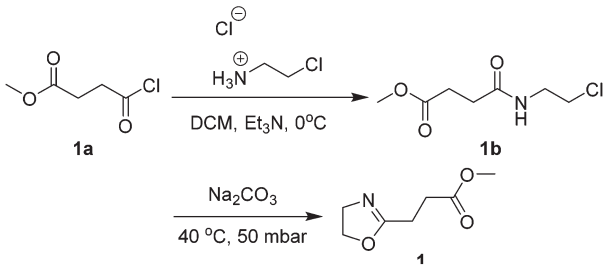

Scheme 2 Synthesis route for preparation of MestOx (1).

and the required removal of the CO_2 that is released. In this work it was found that the yield of this ring-closing reaction can be strongly enhanced by performing it on a rotary evaporator at 40 °C under reduced pressure with sodium carbonate powder. The rotation of the reaction mixture improves the mixing of the salt while the reduced pressure and the enlarged liquid–air surface of the film in the flask facilitates CO_2 removal. The formed MestOx was purified and dried by double distillation over barium oxide leading to 69% yield (57% overall yield).

After preparation of the MestOx monomer, its homopolymerisation was investigated and compared to MeOx and EtOx. Therefore, the polymerisation kinetics were determined using previously optimized polymerisation conditions, namely at 140 °C under microwave irradiation with methyl *p*-toluenesulfonate (MeOTs) as initiator, acetonitrile (CH_3CN) as solvent and 3 M monomer concentration with a [M]/[I] ratio of 100.[25] The first order kinetic plots for MestOx, MeOx and EtOx are shown in Fig. 1 revealing linear first order kinetics for all monomers, indicating a constant concentration of propagating species in time and, thus, the absence of termination reactions. Each data point represents a separate polymerisation indicating the good reproducibility. The livingness of the CROP of these homopolymerisation was confirmed by a linear increase of the number average molecular weight (M_n) with conversion as well as the low dispersities of the resulting polymers ($Đ$ < 1.16, SI Fig. S1†).

The propagation rate constants (k_p) for the homopolymerisations were calculated from the slope of the kinetic plots in

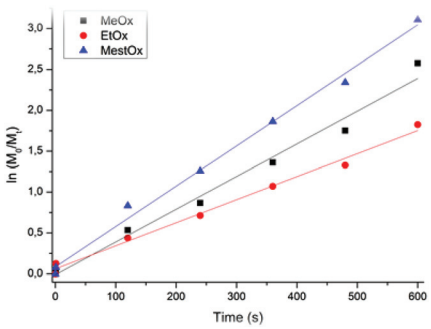

Fig. 1 First order kinetic plot for homopolymerisation of MeOx, EtOx and MestOx (CH_3CN as solvent; 140 °C under microwave irradiation; [M] = 3 M; MeOTs as initiator; [M]/[I] = 100).

Table 1 Propagation rate constants (10^{-3} L mol^{-1} s^{-1}, 140 °C) obtained for the MeOx, EtOx and MestOx homopolymerisations

Monomer	k_p
MeOx	133 ± 4
EtOx	99 ± 3
MestOx	171 ± 4

Fig. 1 and are summarized in Table 1. The k_p's obtained for the homopolymerisations of MeOx and EtOx are in good agreement with previously reported values.[26] MestOx, however, revealed a significantly faster polymerisation with a k_p of 0.171 l mol^{-1} s^{-1}. This fast propagation might be related to the activation of the chain ends and/or stabilization of the transition state by nearby MestOx residues as will be discussed in more detail further on. This mechanism is also indirectly supported by literature,[27] Saegusa and Ikeda showed that the first monomer addition to the oxazolinium cation formed during initiation ($k_{p,1}$) is the rate determining step. After this the propagation rate (k_p) dramatically increases proposedly due to the interaction of the carbonyl of the penultimate unit with the oxazolinium ring, resulting in the stabilisation of the transition state and shift towards the more reactive species. The MestOx has an additional carbonyl group that enhances this effect.

To further evaluate this intriguing polymerisation behaviour of MestOx, its copolymerisations were studied with MeOx and EtOx. Herein, MestOx was copolymerized with MeOx or EtOx, both with a monomer to monomer ratio ($M_1 : M_2$) of 50 : 50 using the same conditions as for the homopolymerisations. Commonly the copolymerisation of different 2-oxazoline monomers follows the same relative order of monomer incorporation as the corresponding homopolymerisations of the individual monomers;[28–31] the only reported exception being the copolymerisation of 2-butyl-4-ethyl-2-oxazoline with 2-phenyl-2-oxazoline ascribed to steric constraints.[32] Remarkably, the first order kinetic plots for the copolymerisation of MestOx with MeOx or EtOx also revealed that MeOx or EtOx is incorporated faster than the MestOx, which is the reversed order compared to the homopolymerisations (Fig. 2). Nonetheless, the linearity of the first order kinetic plots in combination with a linear increase of M_n with conversion and low $Đ$ indicate that the copolymerisations also proceed in a living manner (Fig. 3; ESI Fig. S2 and S3†). A closer look at the first order kinetic plot of the MeOx-MestOx copolymerisation (Fig. 2A) reveals that MeOx reacted almost twice as fast in the copolymerisation (k_p = 244 × 10^{-3} L mol^{-1} s^{-1}, Table 2) compared to its homopolymerisation (k_p = 133 × 10^{-3} L mol^{-1} s^{-1}) while MestOx is remarkably slower in the copolymerisation (k_p = 89 × 10^{-3} L mol^{-1} s^{1}) compared to its homopolymerisation (k_p = 171 × 10^{-3} L mol^{-1} s^{1}). The same trend is also observed for the EtOx-MestOx copolymerisation (Fig. 2B, Table 2), confirming that the presence of MestOx accelerates the polymerisation of the MeOx or EtOx comonomer. This observation is in agreement with the proposed chain end activation and/or transition state stabilization mechanisms, as both MeOx/EtOx and

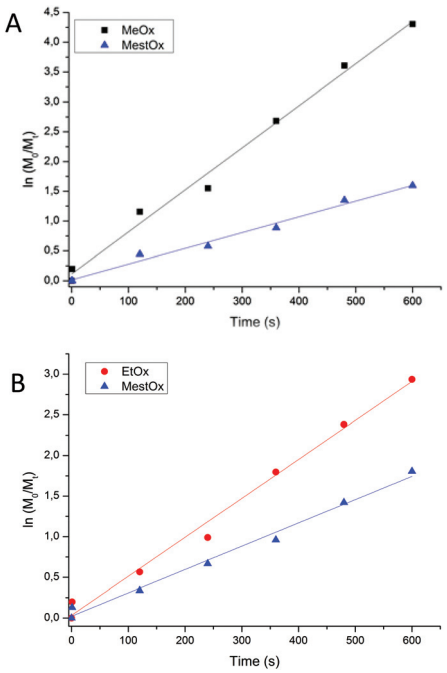

Fig. 2 First order kinetic plot for copolymerisation of (A) MeOx and MestOx and (B) EtOx and MestOx.

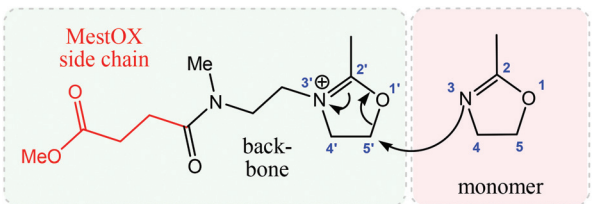

Fig. 3 Schematic representation of the MeOx propagation step in the presence of a nearby MestOx residue.

Table 2 Propagation rate constants (10^{-3} L mol^{-1} s^{-1}, 140 °C) and apparent reactivity ratios obtained for the copolymerisations of MestOx with MeOx and EtOx

Monomer 1	Monomer 2	$k_{p,1}$	$k_{p,2}$	$r_{1,app}$ (k_1/k_2)	$r_{2,app}$ (k_2/k_1)
MeOx	MestOx	244 ± 6	89 ± 3	2.74	0.37
EtOx	MestOx	162 ± 4	97 ± 3	1.67	0.60

MestOx residues are present in the living chain. Hence, nearby MestOx residues will lower the kinetic barrier for the incorporation of both monomers in the copolymerisation. However, the incorporation of MeOx or EtOx is favoured over MestOx, due to lower nucleophilicity of the MestOx monomer (see further).

Despite the reversal in monomer incorporation order, it is interesting that the copolymerisation of MestOx with MeOx or EtOx leads to faster incorporation of MeOx or EtOx followed by slower incorporation of MestOx. From the ratios of the k_p's of the individual monomers during the copolymerisations, the apparent reactivity ratios were estimated,[33] especially for MeOx-MestOx indicating the spontaneous formation of a gradient copolymer structure (Table 2). The average distribution of the monomers along the polymer chain was also calculated from the kinetic plots and are visualised in the ESI Fig. S5A and B† demonstrating the formation of gradient copolymer structures.

In an effort to rationalize the faster incorporation of MeOx into the copolymer chains, the copolymerisation of MeOx and MestOx was further investigated by means of a DFT study (Fig. 3).[34] A population analysis was conducted to compare relative nucleophilicities and reactivities of the two monomers. Furthermore, the MeOx propagation step was modelled in the presence of a nearby MestOx residue to better understand the rate enhancing effects. All geometry optimizations and population analyses were performed at the M06-2X/6-31+G(d,p) level of theory[35] utilizing the Gaussian 09 program package.[36] Further computational details can be found in the ESI.†

Hirshfeld-I (HI)[37] charges were calculated for isolated MeOx and MestOx monomers as well as for the *N*-methyl MeOx and *N*-methyl MestOx oxazolinium cations (Table 3). The nitrogen atom is shown to be more negative in MeOx than in MestOx, indicating a slightly higher nucleophilicity and reactivity towards the living chain, in line with the observed MeOx/MestOx copolymerisation kinetics. In the MestOx$^+$ cation, the side chain prefers to interact with the ring (ΔG = 6.7 kJ mol^{-1}, Fig. 4) causing a slight change in the electrophilicity of the C5′ atom (Table 3).

In order to understand the effect of the nearby MestOx residue, the MeOx propagation step was modelled as a methyl-terminated MestOx-MeOx$^+$ living chain attacked by a MeOx monomer (Fig. 3). HI charges were calculated for pre-reactive complexes (PRCs, Table 4) of three transition states (see

Table 3 HI charges (M06-2X/6-31+G(d,p)) in isolated MeOx and MestOx monomers and *N*-methyl oxazolinium cations

Monomers	O1	C2	N3	C4	C5
MeOx	−0.395	0.671	−0.577	−0.026	0.083
MestOx	−0.395	0.650	−0.567	−0.027	0.083
Cations	**O1′**	**C2′**	**N3′**	**C4′**	**C5′**
MeOx$^+$	−0.279	0.707	−0.132	−0.119	0.041
MestOx$^+$ (interacting)	−0.292	0.708	−0.137	−0.123	0.047
MestOx$^+$ (extended)	−0.266	0.683	−0.137	−0.118	0.040

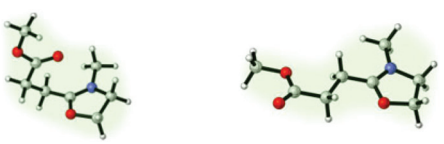

interacting (0.0 kJ/mol) **extended** (6.7 kJ/mol)

Fig. 4 Interacting and extended MestOx$^+$ cation (M06-2X/6-31+G(d,p), relative Gibbs free energies at 140 °C and 1 atm, energy refinement with IEF-PCM in acetonitrile (ε = 35.688)).

Table 4 HI charges (M06-2X/6-31+G(d,p)) in pre-reactive complexes PRC1-3

	O1	C2	N3	O1′	C2′	N3′	C5′
PRC1	−0.367	0.715	−0.626	−0.306	0.695	−0.169	0.063
PRC2	−0.356	0.703	−0.634	−0.292	0.752	−0.203	0.060
PRC3	−0.366	0.701	−0.624	−0.306	0.751	−0.204	0.071

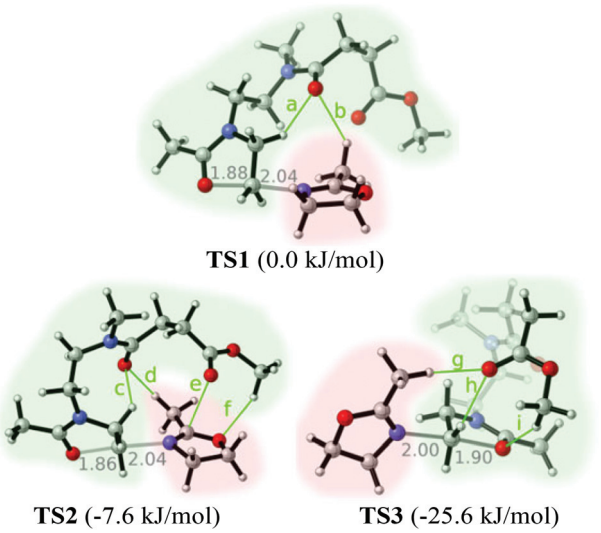

Fig. 5 Transition state geometries for the MeOx propagation step in the presence of a nearby MestOx residue (interactions indicated in green, distances of critical bonds in Å, M06-2X/6-31+G(d,p), relative Gibbs free energies at 140 °C and 1 atm, energy refinement with IEF-PCM in acetonitrile (ε = 35.688)).

further, Fig. 5). Charges on the electrophilic C5′ carbon atom of the oxazolinium cation are shown to be considerably more positive ((+0.060)–(+0.071)) in the PRC's than in the isolated $MeOx^+$ cation (+0.041, Table 3). Furthermore, the nucleophilic N3 nitrogen atom of the attacking monomer is also shown to be more negative ((−0.624)–(−0.634)) in the pre-reactive complex than in the isolated MeOx monomer (−0.577, Table 3). Hence, the interactions of the nearby MestOx side chain induce both an increase in the electrophilicity of the oxazolinium chain end and an increase in the nucleophilicity of the attacking monomer. Three unique transition states (Fig. 5), which differ in the orientation of the MestOx side chain, were identified. Inter- and intra-molecular interaction energies (ΔE_{int}) were determined by natural bond orbital (NBO)[38] analyses (see ESI†).

In TS1, the MestOx side chain adopts a relatively extended conformation. The only apparent intermolecular interaction is between the backbone carbonyl-*O* and the methyl group of the monomer. In TS2, the MestOx residue interacts closely with the attacking MeOx monomer. MestOx side chain carbonyl-*O* coordinates toward the monomer C2′, effectively stabilizing the charge formation in the transition state (ΔE_{int}(e) = 15.8 kJ mol^{-1}), hence lowering the barrier and increasing the propagation rate. Additionally, an intermolecular interaction takes place between the monomer O1 and the MestOx methoxy side chain (ΔE_{int}(f) = 15.9 kJ mol^{-1}), potentially increasing the electron density on N3 and further activating the nucleophile. Both interactions originating from a nearby MestOx residue serve to accelerate the MeOx propagation. In TS3, the side chain of the MestOx residue is more densely packed around the cationic ring moiety and does not extend toward the MeOx monomer as in TS2. The MestOx carbonyl-*O* interacts with oxazolinium ion (ΔE_{int}(h) = 11.2 kJ mol^{-1}) inductively lowering the electron density on C5′, hence activating the chain end and further lowering the barrier for TS3. As a result, TS3 (ΔG = −25.6 kJ mol^{-1}) is more stable than TS2 (ΔG = −7.6 kJ mol^{-1}), and both are more stable than TS1, which lacks interactions with the MestOx side chain.

Conclusions

MestOx was successfully synthesized with an overall yield of 57% *via* the reaction of an acid chloride with 2-chloroethylamine and subsequent ring closure with powderous sodium carbonate under reduced pressure using a rotary evaporator. Homopolymerisation kinetic studies unexpectedly revealed a higher k_p for MestOx compared to MeOx and EtOx while a reversal of monomer incorporation order was found for the copolymerisation of MestOx with MeOx or EtOx, yielding gradient copolymer structures with a gradual change in monomer composition from MeOx or EtOx to MestOx. Density functional theory calculations show that MeOx is a better nucleophile than MestOx, leading to a faster incorporation of MeOx during copolymerisations. Moreover, MestOx residues in a living polymer chain can stabilize the propagation transition state and increase k_p for MeOx, relative to MeOx homopolymerisations. Future work will focus on the variation of the spacer between the oxazoline ring and the methyl ester as well as variation of polymerization temperature to further evaluate this transition state stabilisation mechanism.

Acknowledgements

The computational resources used in this work were provided by Stevin Supercomputer Infrastructure Ghent University (Belgium), the Hercules Foundation, and the Flemish Government – department EWI. V.V.S. and R.H. acknowledge the Belgian Program on Interuniversity Attraction Poles initiated by the Belgian State, the Prime Minister's office (P7/05) and the IWT for support *via* the Strategic Basic Research program (SBO-120049). P.B, and J.H. acknowledge the Polymer Innovation Program (PIPM10006, General adhesive Tissue Tape). All authors acknowledge the Special Research Fund of Ghent University; in particular PB for a joint PhD fellowship.

Notes and references

1 R. Hoogenboom, *Angew. Chem., Int. Ed.*, 2009, **48**, 7978–7994.

2 S. Zalipsky, C. B. Hansen, J. M. Oaks and T. M. Allen, *J. Pharm. Sci.*, 1996, **85**, 133–137.
3 R. Luxenhofer, Y. Han, A. Schulz, J. Tong, Z. He, A. V. Kabanov and R. Jordan, *Macromol. Rapid Commun.*, 2012, **33**, 1613–1631.
4 T. Kagiya, S. Narisawa, T. Maeda and K. Fukui, *J. Polym. Sci., Part B: Polym. Lett.*, 1966, **4**, 441–445.
5 W. Seeliger, E. Aufderhaar, W. Diepers, R. Feinauer, R. Nehring, W. Thier and H. Hellmann, *Angew. Chem., Int. Ed. Engl.*, 1966, **5**, 875–888.
6 D. A. Tomalia and D. P. Sheetz, *J. Polym. Sci., Part A1*, 1966, **4**, 2253–2265.
7 T. G. Bassiri, A. Levy and M. Litt, *J. Polym. Sci., Part B: Polym. Lett.*, 1967, **5**, 871–879.
8 M. W. M. Fijten, C. Haensch, B. M. van Lankvelt, R. Hoogenboom and U. S. Schubert, *Macromol. Chem. Phys.*, 2008, **209**, 1887–1895.
9 B. Guillerm, S. Monge, V. Lapinte and J. J. Robin, *Macromol. Rapid Commun.*, 2012, **33**, 1600–1612.
10 R. Chapman, P. J. M. Bouten, R. Hoogenboom, K. A. Jolliffe and S. Perrier, *Chem. Commun.*, 2013, **49**, 6522–6524.
11 G. Volet, T. X. Lav, J. Babinot and C. Amiel, *Macromol. Chem. Phys.*, 2011, **212**, 118–124.
12 E. Rossegger, V. Schenk and F. Wiesbrock, *Polymers*, 2013, **5**, 956–1011.
13 A. Levy and M. Litt, *J. Polym. Sci., Part A1*, 1968, **6**, 1883–1894.
14 M. T. Zarka, O. Nuyken and R. Weberskirch, *Chem. – Eur. J.*, 2003, **9**, 3228–3234.
15 T. Kotre, M. T. Zarka, J. O. Krause, M. R. Buchmeiser, R. Weberskirch and O. Nuyken, *Macromol. Symp.*, 2004, **217**, 203–214.
16 J. C. Rueda, S. Zschoche, H. Komber, F. Krahl, K. F. Arndt and B. Voit, *Macromol. Chem. Phys.*, 2010, **211**, 706–716.
17 S. Zschoche, J. C. Rueda, M. Binner, H. Komber, A. Janke, K. F. Arndt, S. Lehmann and B. Voit, *Macromol. Chem. Phys.*, 2012, **213**, 215–226.
18 J. C. Rueda, E. Campos, H. Komber, S. Zschoche, L. Haussler and B. Voit, *Des. Monomers Polym.*, 2014, **17**, 208–216.
19 Y. Liu, Y. Wang, Y. F. Wang, J. Lu, V. Pinon and M. Weck, *J. Am. Chem. Soc.*, 2011, **133**, 14260–14263.
20 C. Taubmann, R. Luxenhofer, S. Cesana and R. Jordan, *Macromol. Biosci.*, 2005, **5**, 603–612.
21 A. Gress, A. Volkel and H. Schlaad, *Macromolecules*, 2007, **40**, 7928–7933.
22 A. M. Kelly, A. Hecke, B. Wirnsberger and F. Wiesbrock, *Macromol. Rapid Commun.*, 2011, **32**, 1815–1819.
23 A. Mero, G. Pasut, L. D. Via, M. W. M. Fijten, U. S. Schubert, R. Hoogenboom and F. M. Veronese, *J. Controlled Release*, 2008, **125**, 87–95.
24 R. Hoogenboom, *WO* 2013103297A1, 2013.
25 F. Wiesbrock, R. Hoogenboom, C. H. Abeln and U. S. Schubert, *Macromol. Rapid Commun.*, 2004, **25**, 1895–1899.
26 R. Hoogenboom, M. W. M. Fijten, H. M. L. Thijs, B. M. Van Lankvelt and U. S. Schubert, *Des. Monomers Polym.*, 2005, **8**, 659–671.
27 T. Saegusa and H. Ikeda, *Macromolecules*, 1973, **6**, 808–811.
28 R. Hoogenboom, H. M. L. Thijs, M. W. M. Fijten, B. M. van Lankvelt and U. S. Schubert, *J. Polym. Sci., Part A: Polym. Chem.*, 2007, **45**, 416–422.
29 R. Hoogenboom, F. Wiesbrock, M. A. M. Leenen, M. van der Loop, S. F. G. M. van Nispen and U. S. Schubert, *Aust. J. Chem.*, 2007, **60**, 656–661.
30 S. Huber and R. Jordan, *Colloid Polym. Sci.*, 2008, **286**, 395–402.
31 J.-S. Park and K. Kataoka, *Macromolecules*, 2006, **39**, 6622–6630.
32 H. M. L. Lambermont-Thijs, M. W. M. Fijten, A. J. van der Linden, B. M. van Lankvelt, M. M. Bloksma, U. S. Schubert and R. Hoogenboom, *Macromolecules*, 2011, **44**, 4320–4325.
33 J. E. Puskas, K. B. McAuley and S. W. P. Chan, *Macromol. Symp.*, 2006, **243**, 46–52.
34 H. Goossens, S. Catak, M. Glassner, V. R. de la Rosa, B. D. Monnery, F. De Proft, V. Van Speybroeck and R. Hoogenboom, *ACS Macro Lett.*, 2013, **2**, 651–654.
35 Y. Zhao and D. G. Truhlar, *Theor. Chem. Acc.*, 2008, **120**, 215–241.
36 M. J. Frisch, *et al.*, *Gaussian 09*, *Revision B.01*, Gaussian, Inc., Wallingford, CT, 2010.
37 T. Verstraelen, V. Van Speybroeck and M. J. Waroquier, *J. Chem. Phys.*, 2009, **131**, 044127.
38 A. E. Reed, L. A. Curtiss and F. Weinhold, *Chem. Rev.*, 1988, **88**, 899–926.

